Biogeosciences Discuss., 7, 6847–6887, 2010
www.biogeosciences-discuss.net/7/6847/2010/
doi:10.5194/bgd-7-6847-2010

Biogeosciences Discussions

Temporal and spatial variations of soil carbon dioxide, methane, and nitrous oxide fluxes in a Southeast Asian tropical rainforest

M. Itoh[1,2], Y. Kosugi[3], S. Takanashi[4], Y. Hayashi[3], S. Kanemitsu[3,5], K. Osaka[6], M. Tani[3], and A. R. Nik[7]

[1]Center for Ecological Research, Kyoto University, Shiga 520-2113, Japan
[2]Japan Society for the Promotion of Science, Tokyo 102-8471, Japan
[3]Graduate School of Agriculture, Kyoto University, Kyoto 606-8502, Japan
[4]Forestry and Forest Products Research Institute, Tsukuba, Ibaraki 305-8687, Japan

[5]Sumitomo Forestry Co. Ltd., Tokyo 100-8270, Japan
[6]International Research Center for River Basin Environment, University of Yamanashi, Yamanashi 400-8501, Japan
[7]Forest Research Institute Malaysia, Kepong, Kuala Lumpur 52109, Malaysia

Received: 3 August 2010 – Accepted: 31 August 2010 – Published: 9 September 2010

Correspondence to: M. Itoh (masayukiitoh@yahoo.co.jp)

Published by Copernicus Publications on behalf of the European Geosciences Union.

BGD
7, 6847–6887, 2010

Abstract

To clarify the factors controlling temporal and spatial variations of soil carbon dioxide (CO_2), methane (CH_4), and nitrous oxide (N_2O) fluxes, we investigated these gas fluxes and environmental factors in a tropical rainforest in Peninsular Malaysia. Temporal variation of CO_2 flux in a 2-ha plot was positively related to soil water condition and rainfall history. Spatially, CO_2 flux was negatively related to soil water condition. When CO_2 flux hotspots were included, no other environmental factors such as soil C or N concentrations showed any significant correlation. Although the larger area sampled in the present study complicates explanations of spatial variation of CO_2 flux, our results support a previously reported bipolar relationship between the temporal and spatial patterns of CO_2 flux and soil water condition observed at the study site in a smaller study plot. Flux of CH_4 was usually negative with little variation, resulting in the soil at our study site functioning as a CH_4 sink. Both temporal and spatial variations of CH_4 flux were positively related to the soil water condition. Soil N concentration was also related to the spatial distribution of CH_4 flux. Some hotspots were observed, probably due to CH_4 production by termites, and these hotspots obscured the relationship between both temporal and spatial variations of CH_4 flux and environmental factors. Temporal variation of N_2O flux and soil N_2O concentration was large and significantly related to the soil water condition, or in a strict sense, to rainfall history. Thus, the rainfall pattern controlled wet season N_2O production in soil and its soil surface flux. Spatially, large N_2O emissions were detected in wet periods at wetter and anaerobic locations, and were thus determined by soil physical properties. Our results showed that, even in Southeast Asian rainforests where distinct dry and wet seasons do not exist, variation in the soil water condition related to rainfall history controlled the temporal variations of soil CO_2 flux, CH_4 uptake, and N_2O emission. The soil water condition associated with soil hydraulic properties was also the important controlling factor of the spatial distributions of these gas fluxes.

BGD

7, 6847–6887, 2010

1 Introduction

Tropical rainforests greatly impact global climate by regulating many kinds of trace gas exchange. Whether tropical rainforests function as a sink or a source for biogeochemically produced and consumed global warming gases such as carbon dioxide (CO_2), methane (CH_4), and nitrous oxide (N_2O) needs to be determined. Although studies have investigated soil fluxes of these gases in tropical rainforests, most have examined forests in Amazonia and Central America (e.g., Matson et al., 1990; Steudler et al., 1991; Keller and Reiners, 1994; Riley and Vitousek, 1995; Verchot et al., 1999; Davidson et al., 2000a, 2004, 2008; Vasconcelos et al., 2004), while few have examined Southeast Asian rainforests (e.g., Ishizuka et al., 2002, 2005). The most important environmental difference between Amazonian and Southeast Asian tropical forests with respect to factors affecting CO_2, CH_4, and N_2O fluxes is rainfall patterns, which affect soil water conditions and associated biogeochemical processes. For example, most sites in Amazon rainforests have distinct dry and wet seasons, and therefore the effect of drought stress on gas exchange is an important issue in this region (e.g., Asner et al., 2004). In contrast, Southeast Asian rainforests do not experience distinct dry and wet seasons, although dry and wet periods do exist as part of seasonal fluctuation with considerable variability between years (Tani et al., 2003; Kumagai et al., 2005). Such a difference may affect the production and consumption of trace gases.

Soil CO_2 flux, commonly referred to as soil respiration, is the largest component of net forest CO_2 flux (Raich and Schlesinger, 1992) and accounts for 40 to 70% of total forest respiration (Goulden et al., 1996; Chambers et al., 2004; Ohkubo et al., 2007). Some reports have found no relationship between soil temperature and CO_2 flux in tropical forests (Kursar, 1989; Davidson et al., 2000a). In contrast, soil water condition is considered a key factor controlling CO_2 flux in tropical forests (Davidson et al., 2000a; Hashimoto et al., 2004). Vasconcelos et al. (2004) reported that the decreased CO_2 flux in the dry season and dry season irrigation suppressed the depletion of soil CO_2 flux in Amazonian rainforest. However, Davidson et al. (2008) found no effect of

BGD
7, 6847–6887, 2010

irrigation treatment on CO_2 flux. Thus, the relationship between soil water condition and CO_2 flux is not adequately understood, even in the Amazon where distinct dry and wet seasons occur. These trace gas dynamics should be more thoroughly studied in both Southeast Asian and Amazonian rainforests.

Higher CH_4 and N_2O emissions have been reported during wet periods in Amazonian rainforests (Vasconcelos et al., 2004; Davidson et al., 2004, 2008). Recently Kiese and Butterbach-Bahl (2002), Kiese et al. (2003), and Butterbach-Bahl et al. (2004) investigated temporal variation of these gas fluxes in an Australian tropical rainforest using an automated gas sampling system. They also conducted the same measurements in an African tropical rainforest (Werner et al., 2007). They reported that CH_4 uptake during the dry period was higher than during the wet period (Kiese et al., 2003) and that large pulse emissions of N_2O were observed after the first rainfall events of the wet season (Kiese and Butterbach-Bahl, 2002; Kiese et al., 2003; Butterbach-Bahl et al., 2004; Werner et al., 2007). These studies revealed very detailed time course fluctuations of these gas fluxes. However, such a method cannot be easily applied to multiple sampling points; thus, the spatial distributions of these gas fluxes are still unclear because of the difficulty of multi-point gas flux measurements across a wider area in tropical rainforest. In addition, the information available on gas production below the ground surface and its controlling factors is inadequate. Considering that the soil water condition can affect these gas fluxes, rainfall pattern that affects soil water condition may have an important effect on CH_4 and N_2O.

At our study site in the Pasoh Forest Reserve in Peninsular Malaysia, intensive monitoring of eddy covariance CO_2 flux (Kosugi et al., 2008) and latent and sensible heat fluxes (Takanashi et al., 2010) has been conducted since 2003. Kosugi et al. (2007) found a bipolar pattern of spatial and temporal variation of soil CO_2 flux against soil water content using observations from a 50×50 m (10-m grid) plot. This suggests that not only a physical factor such as the restriction of gas diffusivity with increasing soil water but also a coefficient of some biological or chemical property must be considered. Adachi et al. (2006) reported that spatial variation in CO_2 flux observed near our

BGD
7, 6847–6887, 2010

site (64 m^{-2} quadrat, 28 sampling points) was related to fine root biomass (diameter <1 mm) to a depth of 10 cm. However, whether these results can be scaled to larger areas of flux measurements is unclear. In addition, one report on CH_4 and N_2O fluxes in Pasoh focused on the difference between primary forests and plantations (Yashiro et al., 2008). In the present study, we measured CO_2, CH_4, and N_2O fluxes from the soil surface and soil gaseous concentrations of CO_2, CH_4, and N_2O and examined related environmental factors in a 2-ha plot over a longer sampling period in order to detect longer term trends in these gas fluxes. We focused on the effects of rainfall pattern and soil hydraulic properties, and the associated temporal and spatial variation of soil water condition, on CO_2, CH_4, and N_2O dynamics in this Southeast Asian tropical rainforest.

2 Materials and methods

2.1 Study sites

The study was conducted in the Pasoh Forest Reserve (2°59′ N, 102°18′ E; Fig. 1a) of the Forest Research Institute Malaysia (FRIM) in Peninsular Malaysia. The core area (600 ha) of the reserve is primary lowland mixed dipterocarp forest, consisting of various species of *Shorea* and *Dipterocarpus*. The height of the continuous canopy is approximately 35 m, but some emergent trees exceed 45 m. The soil type around our observation plot is Haplic Acrisol according to FAO classifications. The A horizon is thin (0–5 cm, Yamashita et al., 2003), and lateritic gravels are abundant below 30 cm (Soepadmo, 1978; Yamashita et al., 2003). The area has gently undulating topography. Topographic details and a fetch analysis were recently reported by Takanashi et al. (2010). The soil gas flux observation site has been described in more detail by Kosugi et al. (2008).

Mean annual rainfall is 1804 mm (1983–1997; Tani et al., 2003), less than in other regions of Peninsular Malaysia (Noguchi et al., 2003). Rainfall peaks from March to May and October to December, and occurs mostly from late afternoon to night (Kosugi et al., 2008).

BGD
7, 6847–6887, 2010

2.2 Observations

2.2.1 Sampling points and dates

A 100 × 200-m plot (2 ha-plot) was established near the tower within the 6-ha long-term ecological research plot established by Niiyama et al. (2003; Fig. 1b). The 2-ha plot slopes gently from the flux measurement tower (southeast) to the northwest (Fig. 1b). Flux measurements were made at 15 points along the frame of the 2 ha-plot on 20 August 2006 and at 39 points by adding 24 subpoints as described in Fig. 1c (by adding four chambers each at points 1, 3, 5, 11, 13, and 15) from March 2007 to March 2009 (Fig. 1c).

Soil CO_2 and CH_4 flux measurements were conducted on 20 August 2006, on 3 and 7 March and 12 and 16 December in 2007, on 6 March, 9 June, and 13 October in 2008, and on 9 March 2009. N_2O flux measurements were conducted only on 20 August 2006, 3 March and 12 and 16 December 2007, 9 June and 13 October 2008, and 9 March 2009. Gas flux measurements, soil temperature, and soil water content adjacent to each chamber were measured at all points between about 09:00 and 13:00 local time. No rainfall occurred during the point observations.

2.2.2 CO_2 flux measurements

CO_2 flux was measured using an infrared gas analyzer (IRGA, LI-820 or LI-840, LI-COR, Lincoln, NE, USA) equipped with a closed dynamic chamber system made of PVC. The collars of the chambers, which had an internal diameter of 13 cm and a height of 16 cm, had been earlier inserted 3–5 cm into the soil. The methods of CO_2 flux measurement were described in detail by Kosugi et al. (2007). After the chamber was closed and the increased CO_2 concentration in the chamber had stabilized (approximately 30 s after the chamber top had been placed on the soil collar), the CO_2 concentration was recorded for about 90 s; CO_2 flux was calculated from the increase in CO_2 concentration using a linear regression of the linear section of the record. We used

BGD
7, 6847–6887, 2010

brief measurement periods (90 s), and linearity was checked for each measurement to avoid noise due to pressure artifacts or disturbance of diffusion gradients (Davidson et al., 2002). The zero and span of the IRGA were calibrated in the laboratory before and after each observation campaign.

2.2.3 CH_4 and N_2O flux measurements

The CH_4 and N_2O fluxes were measured in the field using a static closed-chamber method. We used the same chamber collars used for measuring CO_2 flux. Gas samples for CH_4 and N_2O concentration measurements were taken at almost the same time as the CO_2 flux measurements. The lid of the chamber was closed during gas sampling. Each chamber was equipped with a silicon septum to allow samples to be taken using a syringe. Samples for CH_4 and N_2O analysis were collected four times within 30 min from each chamber. The samples were immediately transferred to 10-mL evacuated injection vials and crimp-sealed with a butyl rubber stopper.

For gas samples obtained between 20 August 2006 and 16 December 2007, the CH_4 concentrations were determined using a gas chromatograph (GC: GC-14BPF; Shimadzu, Kyoto, Japan) equipped with a flame ionization detector (FID). For N_2O samples obtained in the same period, concentrations were measured using a gas chromatograph (GC-8A, Shimadzu) equipped with a ^{63}Ni electron capture detector (ECD). For gas samples obtained on 9 June and 13 October 2008 and 9 March 2009, the concentrations of CH_4 and N_2O were determined using an automated gas chromatography system equipped with a FID, an ECD, and a thermal conductivity detector (TCD) (Sudo, 2006). The CH_4 and N_2O fluxes were calculated from linear regressions of concentration versus time curves from the chambers. Positive fluxes indicate the emission of gas from the soil to the atmosphere. Negative fluxes indicate a net uptake of gas from the atmosphere by the soil.

BGD
7, 6847–6887, 2010

2.2.4 Gas concentrations in the soil profile

To measure the soil gas concentrations of CO_2, CH_4, and N_2O, triplicate soil gas samples were collected from 3 March 2007 to 9 March 2009 from five points in the 2-ha plot (double circles in Fig. 1c) (depth: 10, 20, 30, and 50 cm). Soil gas sampling was conducted on the same day as gas flux measurement. For flux measurements conducted in December 2007, soil gas was only sampled once. The ambient gases were also sampled in triplicate. The soil gas sampling tubes, made of stainless steel (outer diameter: 2.5 mm, inner diameter: 1 mm), were inserted vertically into the soil at each soil depth, and the top end of each tube was closed with a rubber septum. Each sample was immediately transferred to a 30-ml evacuated injection vial and crimp-sealed with a butyl rubber stopper. The CH_4 and N_2O concentrations were measured by gas chromatography (as described in Sect. 2.2.3). Soil gas CO_2 concentrations for the samples obtained between 20 August 2006 and 16 December 2007 were measured by a GC (GC-8APT, Shimadzu) equipped with a TCD. For gas samples obtained on 9 June and 13 October 2008, and 9 March 2009, the CO_2 concentration was also determined with an automated gas chromatography system (Sudo, 2006).

2.2.5 Environmental conditions

Soil temperature was measured at the same time as gas flux with a thermistor (Thermo Recorder RT-10 or RT-11, Espec Mic Corp., Aichi, Japan) at a depth of 2 cm and adjacent to each chamber. Soil water content was measured with a HydroSense Soil Water Content Measurement System (CS-620, Campbell Scientific, Inc., Logan, UT, USA) at a depth of 0–12 cm and at three points very close to each chamber, but not in the chamber, to prevent disturbance. In addition to these manual measurements, soil temperature and water content were measured continuously at three points near the flux observation tower (Fig. 1c) at 10-min intervals. Soil temperature was measured at a depth of 2 cm with three thermistors (model 107, Campbell Scientific, Inc.). Soil water content was measured at depths of 10, 20, and 30 cm with nine water content re-

BGD
7, 6847–6887, 2010

flectometers (CS-615 or CS-616, Campbell Scientific, Inc.). These data were recorded using a data logger (CR-10X, Campbell Scientific, Inc).

Soil pH (H_2O) was measured with a glass electrode using a 1:2.5 soil to water ratio in March 2007 at 15 points (the central sampling points) for a soil depth of 0–5 cm. Soil pH (H_2O) was also measured for soil depths of 0, 10, 20, and 30 cm (and 50 cm at point 15) at grid points 5 and 15. Soil mineral samples were collected at depths of 0–5 cm at gas flux measurement points on all sampling days (at the central 15 points in August 2006 and March 2007 and otherwise at all 39 points. In March 2007, soil samples were collected for the 0 to 50 cm depth at points 1, 5, and 15. Samples were obtained in duplicate by hand auger at point 1 and in triplicate by digging a hole at points 5 and 15. Soils were sieved through a 2-mm mesh sieve to remove coarse fragments, and then homogenized. Total N and C concentrations in the soil samples were measured using the combustion method (Bremner, 1996) in an NC-analyzer (Sumigraph NCH-22, Smika Chemical Analysis Service Ltd., Osaka, Japan).

Root biomass samples were collected in March, June, and October 2008 and September 2009 at the 39 gas flux measurement points. In March and June 2008, duplicate soil samples were collected using thin-walled steel samplers with a volume of 100 cm^3 (inner diameter: 5 cm, height: 5.1 cm). In October 2008 and September 2009, the soil just below the flux chambers (depth: 0–5 cm; from a 13-cm diameter area, equal to the diameter of the chamber) was sampled and the chambers were re-located to nearby positions. Roots were sorted from the cores by hand. Live tree roots were placed into two diameter classes: coarse root biomass (diameter >1 mm) and fine root biomass (<1 mm).

We collected undisturbed soil samples at depths of 0–5 cm at points 1–15 using thin-walled steel samplers with a volume of 100 cm^3 (inner diameter: 5 cm, height: 5.1 cm). Undisturbed soil samples were also collected in triplicate at depths of 0–5, 5.0–10.0, 17.5–22.5, 27.5–32.5, and 35.0–40.0 cm at point 5 and at depths of 0–5, 7.5–12.5, 17.5–22.5, 27.5–32.5, and 47.5–52.5 cm at point 15. The sampler with a sharpened edge was inserted vertically into the soil. To ensure sampling with minimum

BGD
7, 6847–6887, 2010

disturbance, we followed the method for collecting undisturbed soil samples described by Grossman and Reinsch (2002). In the laboratory, soil core samples were placed in an aluminum tray and slowly saturated by wetting from the bottom over 24 h. Soil water retention curves were measured by pressure plate methods (Jury et al., 1991) for matric pressure head (ψ) of –5, –10, –20, –30, –50, –70, –100, –200, –500, and –1000 cm. After measuring the water content at ψ = –1000 cm, each sample was oven-dried.

The observed water retention curves were fitted using the lognormal (LN) model for soil retention (Kosugi, 1996). This model is based on the assumption that the soil pore-radius distribution obeys a lognormal distribution and expresses the water retention curve as

$$\theta = (\theta_s - \theta_r) Q\left(\frac{\ln(\psi/\psi_m)}{\sigma}\right) + \theta_r \quad (1)$$

where θ_r and θ_s ($cm^3\ cm^{-3}$) are residual and saturated water content, respectively; ψ_m (cm) is matric pressure head corresponding to the median pore radius; σ represents the width of pore size distribution; and Q denotes the complementary normal distribution function defined as

$$Q(x) = (2\pi)^{-1/2} \int_x^{\infty} \exp\left(-u^2/2\right) du \quad (2)$$

The difference between θ_s and θ_r (i.e., $\theta_e = \theta_s - \theta_r$) represents the total pore volume effective for water retention. In this study, θ_e is referred to as the effective porosity and closely related to gas diffusivity. That is, larger θ_e leads to larger gas diffusivity.

For the application of Eq. (1), for each soil sample, θ_r was fixed at the water content observed at ψ = –1000 cm, which was assumed to be equal to θ_r, and θ_s was fixed at the observed θ_s; the parameters ψ_m, and σ were optimized by minimizing the residual

BGD
7, 6847–6887, 2010

sum of squares computed from

$$\mathrm{RSS} = \sum_{j=1}^{J} \left(\theta^{j}_{\mathrm{obs}} - \theta^{j}_{\mathrm{cal}}\right)^{2} \quad (3)$$

where J is the total number of data points for each soil, $\theta^{j}_{\mathrm{obs}}$ is the jth observed water content for a sample, and $\theta^{j}_{\mathrm{cal}}$ is the calculated water content corresponding to $\theta^{j}_{\mathrm{obs}}$.

We used the mean value of θ_s for the top 0–5 cm of the 15 central sampling points as the representative value of top soil porosity at our site. In this sense, the volumetric soil water content (VSWC) used in the subsequent analyses has a linear relation to water-filled pore space (WFPS), which has been used in other studies. We calculated the WFPS as follows:

$$\mathrm{WFPS}(\%) = \frac{\mathrm{VSWC}(\%)}{\theta_s} \quad (4)$$

Differences between the treatment groups were analyzed using analysis of variance (ANOVA), and specific differences among the groups were analyzed using Tukey's multiple comparison test.

3 Results

3.1 Environmental conditions

3.1.1 Soil chemical and physical properties

The mean soil pH (H_2O) at 0–5 cm depth was 3.86 ± 0.03 (SE) for the 15 points. Soil pH (H_2O) gradually increased with soil depth at two points, from 3.86 ± 0.01 (0 cm) to 4.33 ± 0.05 (30 cm) at point 5 and from 3.79 ± 0.06 (0 cm) to 4.75 ± 0.08 (50 cm) at point 15. Mean values of C and N concentrations in surface soil (0–5 cm) for

BGD
7, 6847–6887, 2010

each sampling occasion ranged from 12.2 to 14.3% and 0.21 to 0.31%, respectively. Depth profiles of C and N concentrations at points 1, 3, and 5, and of soil porosity at points 5 and 15, are shown in Table 1. At both points 5 and 15, the abundance of laterite gravel particles (diameter <1 cm) increased with soil depth. Average soil porosity (saturated water content: θ_s), residual water content (θ_r), effective porosity (θ_e), and ψ_m for 0–5 cm topsoil at the 15 central points was $0.51 \pm 0.01\,cm^3\,cm^{-3}$ (range: 0.44–0.60 $cm^3\,cm^{-3}$), $0.23 \pm 0.01\,cm^3\,cm^{-3}$ (range: 0.14–0.32 $cm^3\,cm^{-3}$), $0.28 \pm 0.02\,cm^3\,cm^{-3}$ (range: 0.20–0.43 $cm^3\,cm^{-3}$), and -17.3 ± 4.1 cm (range: –3.3 to –64.7 cm), respectively.

3.1.2 Temporal variations

Annual rainfall fluctuated between 1450 and 2235 mm during the four years. The site experiences a constant rainy period in November and December, and sometimes has a mild dry period between January and March, and July to October, although the intensities of these dry periods vary. We observed rather dry periods in mid-2006 and 2009, and wet periods at the end of 2007 and in the latter half of 2008. Figure 2 shows that variability of rainfall pattern affected the seasonal and inter-annual variability of VSWC measured near the flux tower. The mean value of VSWC measured at each sampling point was highest in December 2007 (38.8%, range: 27.0–51.0% for the 39 sampling points) and lowest in March 2008 (15.6%, range: 9.0–26.3%); these values are equivalent to WFPS values of 76.0% (range: 52.9–100%) and 30.7% (range: 17.6–51.6%), respectively. Soil temperature was almost constant regardless of the rainfall pattern. We used accumulated rainfall amount and antecedent precipitation index (API_n) as widely used indices to represent both short-term and seasonal trends of rainfall and soil moisture condition. API_n was defined as $\sum_{i=1}^{n} P_i/i$, where P_i is daily precipitation (mm) and i is the number of days leading up to and including the sampling day. We tested n values of 10, 30, and 60 days. Spatially averaged coarse root biomass (diameter >1 mm), fine root biomass (<1 mm), and total root biomass were 103.3–347.79 $g\,m^{-2}$,

BGD
7, 6847–6887, 2010

52.8–95.2 g m^{-2}, and 171.3–400.9 g m^{-2}, respectively. Coarse and total root biomass were highest in October 2008 and fine root biomass was highest in March 2008.

3.1.3 Spatial variations

Maps of spatial variation of soil physical properties (θ_s, θ_r, θ_e, and ψ_m), temporally averaged VSWC, and N concentration at each sampling point are shown in Fig. 3. SigmaPlot ver. 11.0 software (Systat Software Inc., Chicago, IL, USA) was used for graphical analysis of the data. The running average method was used for interpolation of the soil physical parameter data that were observed at the 15 meshed points. The inverse distance method was used for interpolation of the VSWC and soil N concentration data (39 non-meshed data points). Figure 3a suggests that soil porosity (saturated water content: θ_s) was higher along the lines from points 1 to 11 and from points 3 to 4. Figure 3b shows that residual water content (θ_r) was higher at points 1, 9, and 11. Because θ_r indicates the lowest possible soil water content, these points considered to be sustained under wetter conditions than the other points even in driest periods. The effective porosity (θ_e) was low near points 1 and 9, indicating that gas diffusivity should be low at these points (Fig. 3c). These results indicated that the soil was wetter and had lower gas diffusivity at points 1, 9, and 11 than at the other points. Also, ψ_m, which is related to the reciprocal of median pore radius, was smallest at points 1 and 2, indicating that the surface soil pore size was smallest at these points (Fig. 3d). VSWC was usually higher near the line from point 1 to point 5 and low near points 13, 14, and 15 (Fig. 3e). Temporally averaged N concentration was lower in the southwest part of the 2-ha plot and high near point 13 (Fig. 3f).

3.2 CO_2 flux and soil gas CO_2 concentrations

Figure 2 shows the temporal variations in spatially averaged CO_2 flux and CO_2 concentrations. Spatially averaged CO_2 flux in the 2-ha plot ranged from 3.97 (7 March 2007) to 5.67 µmol CO_2 m^{-2} s^{-1} (12 December 2007), with a mean (± SE) value of

BGD
7, 6847–6887, 2010

4.70 ± 0.19 µmol CO_2 m^{-2} s^{-1}. This range was narrower than that previously reported for the site (2.46–6.47 µmol CO_2 m^{-2} s^{-1}; a 36 point average in a 50 × 50 m plot; Kosugi et al., 2007). Both CO_2 flux and soil CO_2 concentrations were high in the wettest period (at the end of 2007). Vertical profiles of soil CO_2 concentrations at five points are shown in Fig. 4a. Soil CO_2 concentration increased with soil depth to a depth of 50 cm at points 1 and 5. The CO_2 concentration was highest at 30 cm depth at points 11, 13, and 15. At point 1, soil CO_2 concentrations were always higher than at the other points. Figure 5a shows the relationships between API_{30} and spatially averaged CO_2 flux at all sampling points for each sampling occasion. Although the relationship was not significant, spatially averaged CO_2 flux was positively related to API_{30} ($p = 0.07$, $r = 0.60$). There was a negative but not significant relationship ($r = -0.26$; $p = 0.10$) between temporally averaged CO_2 flux and VSWC at each sampling point (Fig. 5b). Figure 6a shows a map of the spatial distribution of temporally averaged CO_2 flux. In Fig. 6, the inverse distance method was used for interpolation of the gas flux data (39 non-meshed data points). CO_2 flux was higher near the southwest points 13 and 15. These points are shown in Fig. 5b to have the highest CO_2 fluxes.

3.3 CH_4 flux and soil gas CH_4 concentrations

Temporal variations of spatially averaged CH_4 flux and CH_4 concentrations in soil gas showed that CH_4 flux was usually negative (CH_4 uptake) at the study site and that the variation of both CH_4 flux and soil CH_4 concentration was not great (Fig. 2). High soil gas CH_4 concentrations (about 30 ppmv at point 1, 30 cm depth) were observed only in the wettest period (December 2007). Spatially averaged CH_4 flux ranged from –1.31 (7 March 2007) to 0.02 mg CH_4 m^{-2} d^{-1} (12 December 2007), with a mean value of –0.49 ± 0.15 mg CH_4 m^{-2} d^{-1}. Vertical profiles of soil CH_4 concentrations at points 1, 5, 11, 13, and 15 are shown in Fig. 4b. Soil CH_4 concentration decreased with soil depth and was usually below 1 ppmv at 30 or 50 cm depth at points 5, 13, and 15. At points 1 and 11, CH_4 concentrations increase in the layer of 20–50 cm. Figure 5c shows

BGD
7, 6847–6887, 2010

the relationship between API_{30} and CH_4 flux at all sampling points at each sampling occasion. Although the relationship was not significant, spatially averaged CH_4 flux was positively related to API_{30} ($r = 0.52$, $p = 0.15$). The significant positive relationship between temporally averaged CH_4 flux and VSWC at each sampling point is shown in Fig. 5d ($r = 0.52$, $p < 0.0001$). Figure 6c shows the spatial distribution of temporally averaged CH_4 flux. CH_4 flux was higher near point 2 and in the southwest part of the plot, near point 15.

3.4 N_2O flux and soil gas N_2O concentrations

Temporal variations of spatially averaged N_2O flux and N_2O concentrations in soil gas are shown in Fig. 2. Spatially averaged N_2O flux ranged from 4.88 (7 August 2006) to 309 $\mu g\,N\,m^{-2}\,h^{-1}$ (12 December 2007), with a mean value of $98.9 \pm 40.7\,\mu g\,N\,m^{-2}\,h^{-1}$. Both N_2O flux and N_2O concentrations were high in the wettest period (at the end of 2007). Vertical profiles of soil N_2O concentrations at points 1, 5, 11, 13, and 15 are shown in Fig. 4c. Soil N_2O concentration was higher in deeper soil (30 or 50 cm depth) at points 1 and 11. Figure 5e shows the relationships between API_{30} and N_2O flux at all sampling points at each sampling occasion; a significant positive relationship was found ($r = 0.97$, $p < 0.0005$). A positive but not significant relationship ($r = 0.30$, $p = 0.07$) was found between temporally averaged N_2O flux and VSWC at each sampling point (Fig. 5f). Figure 6e shows the spatial distribution of temporally averaged N_2O flux. N_2O flux was higher near points 9 and 11.

3.5 Hotspots of CO_2, CH_4, and N_2O flux

Hotspots of CO_2, CH_4, and N_2O flux for each sampling occasion were defined as data points with a probability <0.01 of belonging to the 15 or 39 sampling point gas flux data. For this definition, we assumed a normal distribution of gas flux data obtained at each sampling occasion. Threshold values for hotspot fluxes for each gas species and sampling occasion are listed in Table 2. The spatial distribution of event probability of

BGD
7, 6847–6887, 2010

CO_2, CH_4, and N_2O hotspot fluxes are shown in Fig. 6b, d, and f, respectively. Hotspots of CO_2 flux were notable in the northeast part of the plot, at points 13 and 15. CH_4 was also emitted as a hotspot near the southwest part of the plot and near the point 15. N_2O flux were notable in the southwest part of the plot and at points 8 and 11.

4 Discussion

4.1 Temporal variations

4.1.1 CO_2 flux

Kosugi et al. (2007) reported that seasonal variation of soil respiration rate (CO_2 flux) was positively related to soil water content at our site, based on spatially averaged data of CO_2 flux and soil water content from a 50 × 50 m plot. Possible explanations for this relationship were described. Here, we conducted correlation analyses for other environmental factors such as 10-, 30-, and 60-day averaged VSWC, API_{10}, API_{30}, and API_{60}, and 30-day averaged soil temperature. The factors listed in Table 3 were those most significantly correlated to CO_2, CH_4, or N_2O flux. Although the relation was not significant ($r = 0.55$, $p = 0.10$), our results obtained over a larger area (100 × 200 m plot) also found spatially averaged CO_2 flux to be correlated with VSWC, supporting the results of Kosugi et al. (2007) (Table 3a). In addition, soil gas CO_2 concentrations at 10 cm depth were significantly related to VSWC at three of five sampling points, and soil CO_2 concentrations from the surface to deeper zones were correlated with rainfall history (30 day rainfall and API_{30}) (Table 3a). Kursar (1989) found a similar but not significant relationship between soil gas CO_2 concentration and rainfall history. Our results suggest that the positive relationship between seasonal variation of CO_2 flux and soil water content was driven by increased respiration during wet periods, not only in the surface soil layer but also in deeper layers.

BGD
7, 6847–6887, 2010

4.1.2 CH_4 flux

The range of spatially averaged CH_4 flux was very narrow during the sampling periods (–1.31 to 0.02 mg CH_4 m^{-2} d^{-1}). Although the relationship was not significant, CH_4 flux was positively related to VSWC or rainfall history (Table 3b and Fig. 5c). This suggests that CH_4 flux was higher in wetter periods and corresponds with previous reports from Australian tropical rainforests (e.g., Kiese et al., 2003). However, the large sampling area of our study may obscure the relation between CH_4 flux and environmental factors. Soil gas CH_4 concentrations were high in the wettest period in December 2007, but their relationship with environmental factors was barely significant (Table 3b). As a whole, our results showed that the soil at this site functioned as a small net sink for CH_4.

4.1.3 N_2O flux

Table 3c shows the significant relationship between spatially averaged N_2O flux and VSWC. This result corresponds with that found in Costa Rican lowland forest (Keller and Reiner, 1994). In addition, Figs. 2 and 5c indicate that temporal variations in N_2O flux and soil gas N_2O concentrations were regulated by soil water conditions, or, in a strict sense, by the rainfall pattern of preceding days. Even though N_2O flux was only measured seven times, there was a significant relationship between API_{30} and spatially averaged N_2O flux (Fig. 5c and Table 3c; $n = 7$, $F = 69.7$, $r = 0.96$, $p = 0.0004$). Our soil gas N_2O concentration data also strongly supported the relationship between N_2O flux and rainfall history (Table 3c). This relationship between soil water condition and N_2O flux agrees with results from Australian tropical rainforests (Kiese and Butterbach-Bahl, 2002; Butterbach-Bahl et al., 2004), Amazonian tropical rainforest (Davidson et al., 2004), and East African tropical rainforest (Werner et al., 2007), where WFPS was used instead of VSWC as an indicator of soil water condition at the time of gas flux measurement. We found that API_{30}, which includes the recent history of soil water condition, explains the temporal variation of N_2O flux better than measurements of

BGD
7, 6847–6887, 2010

VSWC at sampling time. This suggests that rainfall was the trigger of N_2O production in soil, that this soil N_2O contributed to N_2O emission from the soil surface, and that a time lag of N_2O production or diffusion should be taken into account when predicting N_2O emission from the soil surface. However, we tested such indices of rainfall history and some were found to correlate well with N_2O dynamics. The results indicate that API_{30} may not be the best parameter for all observation sites and that locally appropriate rainfall parameters should be found considering the rainfall pattern or soil hydraulic properties.

4.2 Spatial variation

4.2.1 CO_2 flux

We conducted correlation analyses between temporally averaged CO_2 flux (for all 15 or 39 sampling points) and temporally averaged environmental factors (N and C concentrations, C/N ratio, VSWC, coarse root biomass (diameter >1 mm), fine root biomass (<1 mm), and total root biomass; some of these factors are listed in Table 4). Although most environmental factors were not significantly related to CO_2 flux, a significant negative relationship was found between CO_2 flux and VSWC at each chamber for the 3 and 7 March and 16 December 2007 measurements (Table 4). We found this tendency for temporally averaged CO_2 flux (Fig. 5d; $r = -0.26$; $p = 0.10$). This negative relationship was similar to the results of Kosugi et al. (2007) from the 50 × 50 m plot. However, significant relationships were only found for three of 10 observations, suggesting that our larger study area (2 ha) has greater variation in CO_2 flux than the smaller plot studied by Kosugi et al. (2007). Also, as shown in Table 4, the spatial distribution of CO_2 flux for each gas-sampling occasion was not significantly related to any other environmental factor that we measured. Adachi et al. (2006) reported that spatial variation in CO_2 flux in August 2000 at a site (64 m^{-2} quadrat, 28 sampling points) near ours was related to fine root biomass (diameter <1 mm) to a depth 10 cm; however, we did not find such a relationship in our wider study area. When hotspots of CO_2 flux were ex-

BGD
7, 6847–6887, 2010

cluded, a significant relationship was found between fine root biomass and CO_2 flux at each chamber in March 2008 ($r = 0.38$, $p < 0.05$) and June 2008 ($r = 0.42$, $p < 0.01$), suggesting that root biomass also affects CO_2 flux to a certain degree. Kosugi et al. (2007) reported that the spatial distribution of CO_2 flux was sometimes related to N content in the 50 × 50 m plot. When we included all CO_2 flux data, spatial variation in CO_2 flux did not relate to N concentration. When hotspots were excluded, a significant relationship was found only one out of 10 times, in June 2008 ($r = 0.43$, $p < 0.01$). Our results imply that spatial variation of CO_2 flux in the wider area was complicated by other factors besides N concentration. When considering soil hydraulic properties, soil CO_2 concentration was highest at point 1, where the soil remained wetter (larger θ_r) and gas diffusivity was thought to be lower due to small effective porosity and small soil pore size (smaller ψ_m). However, such spatial heterogeneity of CO_2 production did not correspond with CO_2 flux from the soil surface (Fig. 6a). Besides, the spatial distribution of CO_2 flux was similar to that of CO_2 hotspots (Fig. 6b). Ohashi et al. (2007) reported a high impact of CO_2 hotspots on total soil respiration in a tropical rainforest in Sarawak, Malaysia. They suggested that termite or ant activity may relate to the occurrence of CO_2 hotspots. Termites were reported to contribute considerably to carbon mineralization (Yamada et al., 2005), and termite activity and carbon mineralization were observed at our site (Matsumoto, 1976). Thus, the CO_2 hotspots at our site seem to play a role in the spatial distribution of CO_2 flux and obscure the relationship between CO_2 flux and environmental factors, both temporally and spatially.

4.2.2 CH_4 flux

We also conducted correlation analyses between temporally averaged CH_4 fluxes (for all 39 sampling points) and temporally averaged environmental factors. Among the environmental factors, VSWC has the best correlation with the spatial variations of CH_4 flux (Fig. 5e; $n = 39$, $F = 14.1$, $r = 0.52$, $p < 0.0001$). On three of nine sampling occasions, spatial variation in CH_4 flux was positively related to VSWC (Table 4). Table 4 shows the multiple regression of VWSC and soil N concentration to CH_4 flux. Previous

BGD
7, 6847–6887, 2010

reports of forest floor CH_4 flux have indicated that CH_4 emissions in the high VSWC range may be due to increased methanogenesis (Itoh et al., 2009). Itoh et al. (2009) found that CH_4 production in periods of high temperature can exceed CH_4 oxidation, even in unsaturated temperate forest soils in the Asian monsoon region. The CH_4 emissions observed in the wet period (December, 2007) were probably the result of CH_4 production by methanogenesis. Higher sustained soil CH_4 concentrations at points 1 and 11, where the soil was wetter and had lower gas diffusivity than at other points, support the idea that CH_4 was produced under anaerobic conditions. Alternatively, the limitation of CH_4 oxidation due to the lower gas diffusivity in wet periods (Born et al., 1990; Dörr et al., 1993) may also affect the positive relationship between VSWC and CH_4 flux.

We should also consider the potential contribution of termite emissions to CH_4 production (e.g., Sugimoto et al., 1998a, b). High levels of CH_4 emission were observed at our site under low VSWC conditions (<20%) under which CH_4 production by methanogenesis usually does not stand out in forest soil (Fig. 5d). Thus, it is difficult to discern the effect of termite CH_4 emissions because of the large interspecies variation in emission rates and the difficulty of estimating population size (Cicerone and Oremland, 1988; Fung et al., 1991). Many termite species are found at our site (Abe and Matsumoto, 1979). Some underground mounds and nests of *Dicuspiditermes*, *Microtermes*, and *Homalloterme* were found to produce CH_4 (Sugimoto et al., 1998b). We collected gas samples from some mounds of *Dicuspiditermes*, and found CH_4 concentrations of 6.5 ppm at a depth of 10 cm, 37.7 ppm at 20 cm, and 17.4 ppm at 30 cm on 7 March 2007. This suggests that CH_4 was indeed produced in the termite mounds. Thus, termite emissions should be considered when evaluating CH_4 flux at our site. The high event probability of both CH_4 and CO_2 hotspots in the southwest part of the point 15 indicated the possibility of termite contributions to high emissions of CH_4 and CO_2. However, our results suggested that the spatial variation of CH_4 flux at our site was mainly controlled by soil water conditions, despite the effect of termite CH_4 production. Separating the sites with termite CH_4 production from those without termite

BGD
7, 6847–6887, 2010

production by using isotopic measurements would lead to a better understanding of CH_4 flux in tropical rainforests.

4.2.3 N_2O flux

To clarify the spatial distribution of N_2O flux, we conducted correlation analyses between temporally averaged N_2O flux (for all 39 sampling points) and temporally averaged environmental factors, similar to the analyses for CO_2 flux and CH_4 flux. Among all the environmental factors, soil N concentration showed the best correlation with temporally averaged N_2O flux ($n = 39$, $F = 7.2$, $r = 0.40$, $p = 0.01$). Also, multiple regression analysis using VSWC and surface soil N concentration explained more of the spatial variation in N_2O flux ($n = 39$, $F = 7.7$, $r = 0.55$, $p = 0.002$). Here, temporally averaged VSWC and N concentration were not significantly correlated ($p = 0.32$).

Regarding the spatial variation in N_2O flux at each sampling occasion, few correlations were found between the environmental factors and N_2O flux (Table 4). For two of the seven sampling occasions, multiple regressions between VSWC and N concentration and N_2O flux were significant (Table 4). At point 11, where soil N_2O concentration was higher (Fig. 4), temporally averaged N_2O flux was highest (Fig. 6e) and a hotspot of N_2O flux was often observed (Fig. 6f). At this point, gas diffusivity was lower and the soil was wetter than at the other points (Fig. 3a–e). A similar pattern of small θ_e, large θ_r, and high N_2O flux was also observed at point 9 (Figs. 3b and 6e). These results indicate that the spatial distribution of soil hydraulic properties also affects soil N_2O production and emission from the surface.

We should consider whether N_2O emission is caused by nitrification or denitrification. As reported by Bateman and Baggs (2005), at lower soil water conditions such as 35–60% WFPS, nitrification was considered to be the main process producing N_2O. Some reports have shown a relationship between soil nitrification rate and N_2O flux from tropical soil (as summarized by Ishizuka et al., 2002), suggesting that nitrification is a main factor in N_2O emissions at such sites. At these sites, N_2O flux was as high as 40 $\mu g\,N\,m^{-2}\,h^{-1}$, much lower than our highest measured N_2O emission. Meanwhile,

BGD
7, 6847–6887, 2010

denitrification is increasingly dominant at values >60% WFPS, i.e., under conditions where soils are becoming predominantly anaerobic (Linn and Doran, 1984; Davidson et al., 2000b). Also, Davidson et al. (1993) suggested that denitrification was the dominant source of N_2O during the wet season in a dry tropical forest in Mexico. Although we do not have detailed data of nitrogen dynamics such as inorganic nitrogen levels in soil, a large pulse of N_2O emission was observed in December 2007 during the wettest period at our site. At that time, the soil water condition (WFPS) was 76.0% (range: 52.9–100%) and 70.7% (47.1–96.7%) in the top 0–5 cm of soil on 12 and 16 December, respectively, values high enough to allow denitrification to dominate (Davidson et al., 2000b). These results indicate that denitrification likely dominated at our site during very wet periods. High soil gas N_2O concentrations observed at points 1 and 11, where wetter and anaerobic conditions were sustained, were likely due to denitrification. The production of N_2O from the high rate of denitrification at these wet points must have contributed to the high N_2O emission.

5 Conclusions

Soil CO_2, CH_4, and N_2O fluxes were measured in a Southeast Asian tropical rainforest. Temporal variation of CO_2 flux in our 2-ha plot was positively related to soil water conditions such as volumetric soil water condition (VSWC), rainfall, and rainfall history. Soil gas CO_2 concentrations were also related to rainfall history, suggesting that microbial activity increases during wet periods. Spatially, CO_2 flux was negatively related to VSWC on three of 10 sampling occasions. Other environmental factors such as soil C and N concentrations and root biomass that have been mentioned elsewhere as controlling factors of spatial variation were not consistently related to CO_2 flux. Although the larger area sampled in the present study complicates explanations of spatial variation of CO_2 flux because of increased variability and the occurrence of respiration hotspots, our results support the previously reported bipolar relationship between CO_2 flux and VSWC.

BGD
7, 6847–6887, 2010

CH_4 flux was generally negative with little variation, resulting in the soil at our study site functioning as a CH_4 sink throughout almost the entire observation period. Although not significant, temporal variation of spatially averaged CH_4 flux was related to the soil water condition. Spatial variation of CH_4 flux was positively related to VSWC and rainfall history. We detected some hotspots of CH_4 emission that sometimes corresponded with CO_2 flux hotspots, implying the contribution of termite CH_4 production to net CH_4 flux at our site.

Temporal variation of N_2O flux was large and significantly related to the soil water condition, or, in a strict sense, rainfall history, such as API_{30}. Rainfall history also showed a significant positive relation to soil N_2O concentration. Thus, the rainfall pattern controlled wet season N_2O production and flux. Spatially, N_2O flux was related to both VSWC and soil N concentration. Also, soil N_2O production was higher in wetter and aerobic locations because of soil physical factors. Our results indicate that, under anaerobic conditions, denitrification should contribute to N_2O production at our site. Furthermore, N_2O flux observation periods at tropical rainforest sites should include the wettest period in order to detect the highest levels of N_2O emission.

Variation in soil water condition, which is associated with rainfall history, controls CO_2 flux, CH_4 uptake, and N_2O emission, and, in particular, their temporal variations at our study site. Our results suggest that the effects of rainfall pattern can be seen even in Southeast Asian rainforests where distinct dry and wet seasons do not occur. The soil water condition, in association with soil hydraulic properties, was an important factor controlling the spatial distribution of these gas fluxes at our study site.

Acknowledgements. We thank the Forestry Department of Negeri Sembilan and the director general of the Forest Research Institute Malaysia (FRIM) for granting us permission to work in the Pasoh Forest Reserve. We gratefully acknowledge the staff members of the Hydrology Unit and the Pasoh Station of the FRIM for collecting field data. We also thank a joint research project between FRIM, Putra University, Malaysia (UPM), and the National Institute for Environmental Studies (NIES), Japan. We additionally thank N. Matsuo, K. Tanaka, T. Nakaji, and M. Dannoura, and R. Nakagawa, N. Makita, and A. Kanazawa for their help with gas flux measurements. This work was supported by Grants-in-Aid for Scientific Research (20780117,

BGD
7, 6847–6887, 2010

16658065, PD22-5033), Japan, and the Japan Society for the Promotion of Science (JSPS) Global Centers of Excellence (COE) Program (E-04): In Search of Sustainable Humanosphere in Asia and Africa.

References

Abe, T. and Matsumoto, T.: Studies on the distribution and ecological role of termites in lowland rainforest of West Malaysia. 3. Distribution and abundance of termites in Pasoh Forest Reserve, Jpn. J. Ecol., 29, 337–351, 1979.

Adachi, M., Bekku, Y. S., Rashidah, W., Okuda, T., and Koizumi, H.: Differences in soil respiration between different tropical ecosystems, Appl. Soil Ecol., 34, 258–265, 2006.

Asner, G. P., Nepstad, D., Cardinot, G., and David, R.: Drought stress and carbon uptake in an Amazon forest measured with spaceborne imaging spectroscopy, Proceedings of the National Academy of Sciences of the United States of America, 101, 6039–6044, 2004.

Bateman, E. J. and Baggs, E. M.: Contributions of nitrification and denitrification to N_2O emissions from soils at different water-filled pore space, Biol. Fert. Soils, 41, 379–388, 2005.

Born, M., Dörr, H., and Levin, I.: Methane consumption in aerated soils of the temperate zone, Tells, 42B, 2–8, 1990.

Bremner, J. M.: N-total, in: Methods of soil analysis, Part 3, in: (Soil Sci. Soc. Am. Book Series, No. 5), edited by: Sparks, D. L., Page, A. L., Helmke, P. A., et al., 1085–1121, Soil Sci. Soc. Am. and Am. Soc. of Agron. Madison, Wisconsin, USA, 1996.

Butterbach-Bahl, K., Kock, M., Willibald, G., Hewett, B., Buhagiar, S., Papen, H., and Kiese, R.: Temporal variations of fluxes of NO, NO_2, N_2O, CO_2, and CH_4 in a tropical rain forest ecosystem, Global Biogeochem. Cy., 18, GB3012, doi:10.1029/2004GB002243, 2004.

Cicerone, R. J. and Oremland, R. S.: Biogeochemical aspects of atmospheric methane, Global Biogeochem. Cy., 2, 299–327, 1988.

Chambers, J. Q., Tribuzy, E. S., Toledo, L. C., Crispim, B. F., Higuchi, N., Santos, J. D., Araújo, A. C., Kruijt, B., Nobre, A. D., and Trumbore, S. E.: Respiration from a tropical forest ecosystem: partitioning of sources and low carbon use efficiency, Ecol. Appl., 14, S72–S88, 2004.

Davidson, E. A., Matson, P. A., Vitousek, P. M., Riley, R., Dunkin, K., García-Méndez, G., and Maass, J. M.: Processes regulating soil emissions of NO and N_2O in a seasonally dry tropical forest, Ecology, 74, 130–139, 1993.

BGD

7, 6847–6887, 2010

Davidson, E. A., Verchot, L. V., Henrique Cattânio, J., Ackerman, I. L., and Carvalho, J. E. M.: Effects of soil water content on soil respiration in forests and cattle pastures of eastern Amazonia, Biogeochemstry, 48, 53–69, doi:10.1023/A:1006204113917, 2000a.
Davidson, E. A., Keller, M., Erickson, H. E., Verchot, L. V., and Veldkamp, E.: Testing a conceptual model of soil emissions of nitrous and nitric oxides, BioScience, 50, 667–680, 2000b.
Davidson, E. A., Savage, K., Verchot, L. V., and Navarro, R.: Minimizing artifacts and biases in chamber-based measurements of soil respiration, Agr. Forest Meteorol., 113, 21–37, 2002.
Davidson, E. A., Ishida, F. Y., and Nepstad, D. C.: Effects of an experimental drought on soil emissions of carbon dioxide, methane, nitrous oxide, and nitric oxide in a moist tropical forest, Global Change Biol., 10, 718–730, 2004.
Davidson, E. A., Ishida, F. Y., and Nepstad, D. C.: Effects of an experimental drought and recovery on soil emissions of carbon dioxide, methane, nitrous oxide, and nitric oxide in a moist tropical forest, Global Change Biol., 14, 2582–2590, 2008.
Dörr, H., Katruff, L., and Levin, I.: Soil texture parameterization of the methane uptake in aerated soils, Chemosphere, 26, 697–713, 1993.
Fung, I., John, J., Lerner, J., Matthews, E., Prather, M., Steele, L. P., and Fraser, P. J.: Three-Dimensional Model Synthesis of the Global Methane Cycle, J. Geophys. Res., 96 (D7), 13033–13065, doi:10.1029/91JD01247, 1991.
Goulden, M. L., Munger, J. W., Fan, S. M., Daube, B. C., and Wofsy, S. C.: Measurements of carbon sequestration by long-term eddy covariance: methods and a critical evaluation of accuracy, Global Change Biol., 2, 169–182, 1996.
Grossman, R. B. and Reinsch, T. G.: Core method, in: Methods of Soil Analysis. Part 4 – Physical Methods, edited by: Klute, A., Monograph, 9, ASA and SSSA, Madison, WI, 207–209, 2002.
Hashimoto, S., Tanaka, N., Suzuki, M., Inoue, A., Takizawa, H., Kosaka, I., Tanaka, K., Tantasirin, C., and Tangtham, N.: Soil respiration and soil CO_2 concentration in a tropical forest, Thailand, J. For. Res., 9, 75–79, 2004.
Ishizuka, S., Tsuruta, H., and Murdiyarso, D.: An intensive field study on CO_2, CH_4, and N_2O emissions from soils at four land-use types in Sumatra, Indonesia, Global Biogeochem. Cy., 16, 1049, doi:10.1029/2001GB001614, 2002.
Ishizuka, S., Iswandi, A., Nakajima, Y., Yonemura, S., Sudo, S., Tsuruta, H., and Murdiyarso, D.: The variation of greenhouse gas emissions from soils of various land-use/cover types in Jambi province, Indonesia, Nutr. Cycl. Agroecosys., 71, 17–32, 2005.

BGD
7, 6847–6887, 2010

Itoh, M., Ohte, N., and Koba, K.: Methane flux characteristics in forest soils under an East Asian monsoon climate, Soil Biol. Biochem., 41, 388–395, 2009.
Jury, W. A., Gardner, W. R., and Gardner, W. H.: Water Characteristic Function, in: Soil Physics, 5th Edition, Wiley, New York, 61–67, http://www.amazon.com/Soil-Physics-5th-William-Jury/dp/0471831085/ref=sr_1_6?s=books\&ie=UTF8\&qid=1283734770\&sr=1-6# 1991.
Keller, M. and Reiners, W. A.: Soil-atmosphere exchange of nitrous oxide, nitric oxide, and methane under secondary succession of pasture to forest in the Atlantic lowlands of Costa Rica, Global Biogeochem. Cy., 8, 399–410, 1994.
Kiese, R. and Butterbach-Bahl, K.: N_2O and CO_2 emissions from three different tropical forest sites in the wet tropics of Queensland, Australia, Soil Biol. Biochem, 34, 975–987, 2002.
Kiese, R., Hewett, B., Graham, A., and Butterbach-Bahl, K.: Seasonal variability of N_2O emissions and CH_4 uptake by tropical rainforest soils of Queensland, Australia, Global Biogeochem. Cy. 17, 1043–1055, 2003.
Kosugi, K.: Lognormal distribution model for unsaturated soil hydraulic properties. Water Resour. Res., 32, 2697–2703, 1996.
Kosugi, Y., Mitani, T., Itoh, M., Noguchi, S., Tani, M., Matsuo, N., Takanashi, S., Ohkubo, S., and Nik A. R.: Spatial and temporal variation in soil respiration in a Southeast Asian tropical rainforest, Agr. Forest Meteorol., 147, 35–47, 2007.
Kosugi, Y., Takanashi, S., Ohkubo, S., Matsuo, N., Tani, M., Mitani, T., Tsutsumi, D., and Nik, A. R.: CO_2 exchange of a tropical rainforest at Pasoh in Peninsular Malaysia, Agr. Forest Meteorol., 148, 439–452, 2008.
Kumagai, T., Saitoh, T. M., Sato, Y., Takahashi, H., Manfroi, O. J., Morooka, T., Kuraji, K., Suzuki, M., Yasunari, T., and Komatsu, H.: Annual water balance and seasonality of evapotranspiration in a Bornean tropical rainforest, Agr. Forest Meteorol., 128, 81–92, 2005.
Kursar, T. A.: Evaluation of soil respiration and soil CO_2 concentration in a lowland moist forest in Panama, Plant Soil, 113, 21–29, 1989.
Linn, D. M. and Doran, J. W.: Effect of water-filled pore space on carbon dioxide and nitrous oxide production in tilled and nontilled soils, Soil Sci. Soc. Am. J., 48, 1267–1272, 1984.
Matson, P. A., Vitousek, P. M., Livingston, G. P., and Swanberg, N. A.: Sources of variation in nitrous oxide flux from Amazonian ecosystems, J. Geophys. Res., 95(D10), 16789–16798, doi:10.1029/JD095iD10p16789, 1990.
Matsumoto, T.: The role of termites in an equatorial rain forest ecosystem of West Malaysia. I. Population density, biomass, carbon, nitrogen and calorific content and respiration rate,

BGD
7, 6847–6887, 2010

Oecologia, 22, 153–178, 1976.
Niiyama, K., Kassim, A. R., Iida, S., Kimura, K., Azizi, R., and Appanah, S.: Regeneration of clear-cut plot in a lowland dipterocarp forest in Pasoh Forest Reserve, Peninsular Malaysia, in: Pasoh: Ecology of a lowland rain forest in southeast Asia, edited by: Okuda, T., Manokaran, Y., Matsumoto, Y., Niiyama, K., Thomas, S. C., and Ashton, P. S., Springer-Verlag, Tokyo, 559–568, 2003.
Noguchi, S., Nik, A. R., and Tani, M.: Rainfall characteristics of tropical rainforest at Pasoh Forest Reserve, Negeri Sembilan, Peninsular Malaysia, in: Pasoh : Ecology of a lowland rain forest in southeast Asia, edited by: Okuda T., Manokaran, N., Matsumoto, Y., Niiyama, K., Thomas, S. C., and Ashton, P. S., Springer, Tokyo, 51–58, 2003.
Ohashi, M., Kume, T., Yamane, S., and Suzuki, M.: Hot spots of soil respiration in an Asian tropical rainforest, Geophys. Res. Lett., 34, L08705, doi:10.1029/2007GL029587, 2007.
Ohkubo, S., Kosugi, Y., Takanashi, S., Mitani, T., and Tani, M.: Comparison of the eddy covariance and automated closed chamber methods for evaluating nocturnal CO_2 exchange in a Japanese cypress forest, Agr. Forest Meteorol., 142, 50–65, 2007.
Raich, J. W. and Schlesinger, W. H.: The global carbon dioxide flux in soil respiration and its relationship to vegetation and climate, Tellus, 44B, 81–99, 1992.
Riley, R. H. and Vitousek, P. M.: Nutrient dynamics and nitrogen trace gas flux during ecosystem development in montane rain forest, Ecology, 76, 292–304, 1995.
Soepadmo, E.: Introduction to the Malaysian I. B. P. Synthesis Meetings, The Malayan Nature Journal, 30, 119–124, 1978.
Sudo, S. Method and instrument for measuring atmospheric gas, Industrial Property Digital Library, Patent of Japan (no. 2006-275844), 2006.
Steudler, P. A., Melillo, J. M., Bowden, R. D., Castro, M. S., and Lugo, A. E.: The Effects of natural and human disturbances on soil nitrogen dynamics and trace gas fluxes in a Puerto rican wet forest, Biotropica, 23, 356–363, 1991.
Sugimoto, A., Inoue, T., Kirtibutr, N., and Abe, T.: Methane oxidation by termite mounds estimated by the carbon isotopic composition of methane, Global Biogeochem. Cy., 12, 595–605, 1998a.
Sugimoto, A., Inoue, T., Tayasu, I., Miller, L., Takeichi, S., and Abe, T.: Methane and hydrogen production in a termite-symbiont system, Ecol. Res., 13, 241–257, 1998b.
Takanashi, S., Kosugi, Y., Ohkubo, S., Matsuo, N., Tani, M., and Nik, A. R.: Water and heat fluxes above a lowland dipterocarp forest in Peninsular Malaysia, Hydrol. Process., 24, 472–

BGD
7, 6847–6887, 2010

480, 2010.
Tani, M., Nik, A. R., Ohtani, Y., Yasuda, Y., Sahat, M. M., Baharuddin, K., Takanashi, S., Noguchi, S., Zulkifli, Y., and Watanabe, T.: Characteristics of energy exchange and surface conductance of a tropical rain forest in Peninsular Malaysia, in: Pasoh: Ecology of a lowland rain forest in southeast Asia, edited by: Okuda T., Manokaran, N., Matsumoto, Y., Niiyama, K., Thomas, S. C., Ashton, P. S., Springer, Tokyo, 73–88, 2003.
Vasconcelos, S. S., Zarin, D. J., Capanu, M., Littell, R., Davidson, E. A., Ishida, F. Y., Santos, E. B., Araujo, M. M., Aragao, D. V., Rangel-Vasconcelos, L. G. T., Oliveira, F. A., McDowell, W. H., and Carvalho, C. J. R.: Moisture and substrate availability constrain soil trace gas fluxes in an eastern Amazonian regrowth forest, Global Biogeochem. Cy., 18, GB2009, doi:10.1029/2003GB002210, 2004.
Verchot, L. V., Davidson, E. A., Cattânio, H., Ackerman, I. L., Erickson, H. E., and Keller, M.: Land use change and biogeochemical controls of nitrogen oxide emissions from soils in eastern Amazonia, Global Biogeochem. Cy., 13, 31–46, doi: 10.1029/1998GB900019, 1999.
Werner, C., Kiese, R., and Butterbach-Bahl, K.: Soil-atmosphere exchange of N_2O, CH_4, and CO_2 and controlling environmental factors for tropical rain forest sites in western Kenya, J. Geophys. Res., 112, D03308, doi:10.1029/2006JD007388, 2007.
Yamada, A., Inoue, T., Wiwatwitaya, D., Ohkuma, M., Kudo, T., Abe, T., and Sugimoto, A.: Carbon mineralization by termites in tropical forests, with emphasis on fungus combs, Ecol. Res., 20, 453–460, 2005.
Yamashita, T., Kasuya, N., Kadir, W. R., Chik, S. W., Seng, Q. E., and Okuda, T.: Soil and belowground characteristics of Pasoh Forest Reserve, in: Pasoh: Ecology of a lowland rain forest in southeast Asia, edited by: Okuda T., Manokaran, N., Matsumoto, Y., Niiyama, K., Thomas, S. C., Ashton, P. S., Springer, Tokyo, 89–109, 2003.
Yashiro, Y., Kadir, W. R., Okuda, T., and Koizumi, H.: The effects of logging on soil greenhouse gas (CO_2, CH_4, N_2O) flux in a tropical rain forest, Peninsular Malaysia, Agr. Forest Meteorol., 148, 799–806, 2008.

BGD
7, 6847–6887, 2010

Table 1. Depth profiles of C and N concentrations (Mean ± SE), C/N ratio, and saturated water content (θ_s) and effective porosity (θ_r) (Mean ± SE). Samples for C and N concentrations were obtained in duplicate by hand auger at point 1 and in triplicate by digging a hole at points 5 and 15 in March 2007. Boldface indicates a significant difference between C and N concentrations at points 5 and 15 at the same sampling depth.

Point	Depth (cm)	C conc. (%)	N conc. (%)	C/N	θ_s ($cm^3\,cm^{-3}$)	θ_e ($cm^3\,cm^{-3}$)
1	0–10	2.46 ± 0.51	0.18 ± 0.02	13.9	0.53	0.20
	10.0–20.0	1.14 ± 0.19	0.09 ± 0.00	12.5	NM	NM
	20.0–30.0	0.74 ± 0.16	0.07 ± 0.01	10.1	NM	NM
	30.0–40.0	0.87 ± 0.43	0.08 ± 0.03	11.1	NM	NM
	40.0–50.0	0.56 ± 0.25	0.05 ± 0.01	10.4	NM	NM
5	0–5.0	**4.52 ± 0.26***	**0.31 ± 0.01***	14.6	0.50 ± 0.01	0.36 ± 0.02
	7.5–12.5[a]	1.67 ± 0.08	0.14 ± 0.01	12.0	0.47 ± 0.00	0.33 ± 0.04
	17.5–22.5	1.75 ± 0.19	**0.15 ± 0.01**†	11.8	0.45 ± 0.02	0.35 ± 0.02
	27.5–32.5	**1.11 ± 0.04***	**0.11 ± 0.00**††	10.3	0.45 ± 0.01	0.36 ± 0.02
	35.0–40.0	NM	NM	NM	0.36 ± 0.00	0.23 ± 0.01
15	0–5.0	2.55 ± 0.12	0.18 ± 0.01	14.1	0.48 ± 0.01	0.33 ± 0.06
	7.5–12.5	1.60 ± 0.09	0.13 ± 0.01	11.9	0.43 ± 0.04	0.34 ± 0.06
	17.5–22.5	1.21 ± 0.07	0.11 ± 0.01	11.5	0.43 ± 0.03	0.37 ± 0.02
	27.5–32.5	0.92 ± 0.04	0.09 ± 0.00	10.7	0.42 ± 0.02	0.36 ± 0.02
	47.5–52.5	0.87 ± 0.09	0.08 ± 0.01	10.6	0.34 ± 0.03	0.22 ± 0.04

† $p < 0.05$, †† $p < 0.01$, * $p < 0.005$, and ** $p < 0.001$. [a] Sampling depth for soil porosity was 5.0–10.0 cm. NM: not measured.

BGD
7, 6847–6887, 2010

Table 2. Average gas fluxes and their hotspot threshold values and the number of hotspots on each sampling occasion. Figures in parentheses indicate the number of chambers measured on each sampling occasion.

Gas and measurement date	Average flux	Threshold value of Hotspot	N of hotspots
CO_2 flux	μmol CO_2 m^{-2} s^{-1}	μmol CO_2 m^{-2} s^{-1}	
19 Aug 2006 (15)	4.06	6.76	1
3 Mar 2007 (39)	4.71	7.84	3
7 Mar 2007 (39)	3.97	6.62	4
12 Dec 2007 (39)	5.67	9.43	4
16 Dec 2007 (39)	5.00	8.32	4
6 Mar 2008 (39)	4.12	6.87	3
9 Jun 2008 (39)	4.14	6.89	2
1 Oct 2008 (39)	5.32	8.86	5
9 Mar 2009 (39)	5.22	8.70	4
14 Sep 2009 (39)	4.79	7.97	2
CH_4 flux	mg CH_4 m^{-2} d^{-1}	mg CH_4 m^{-2} d^{-1}	
19 Aug 2006 (15)	−0.29	0.53	2
3 Mar 2007 (39)	−0.15	2.13	6
7 Mar 2007 (39)	−1.31	−0.61	4
12 Dec 2007 (39)	0.02	0.73	6
16 Dec 2007 (39)	−0.37	0.20	2
6 Mar 2008 (39)	−0.93	0.04	5
9 Jun 2008 (39)	−0.27	0.35	8
1 Oct 2008 (39)	−0.26	0.18	6
9 Mar 2009 (39)	−0.87	0.16	3
N_2O flux	μg N m^{-2} h^{-1}	μg N m^{-2} h^{-1}	
19 Aug 2006 (15)	4.88	7.09	4
3 Mar 2007 (39)	16.3	27.3	4
12 Dec 2007 (39)	309	672	5
16 Dec 2007 (39)	131	257	3
9 Jun 2008 (39)	130	388	3
1 Oct 2008 (39)	89.3	210	5
9 Mar 2009 (39)	11.7	18.5	8

BGD
7, 6847–6887, 2010

Table 3. Pearson correlation coefficients and their level of significance between mean **(a)** CO_2, **(b)** CH_4, and **(c)** N_2O fluxes and mean soil gas concentration and environmental conditions during the observation period. Figures in parentheses indicate the number of gas samplings during the observation period. The 30-day rainfall values are the amount of total rainfall in the 30 days leading up to and including the sampling day. The values of volumetric soil water content (VSWC) are average values from nine CS-615/616 sensors at 10, 20, and 30 cm for soil water content at three locations continuously measured near the flux observation tower. These were used as reference values indicating the temporal characteristics of each observation period. Boldface indicates significant correlations.

(a) CO_2	VSWC	Soil temp.	30-day rainfall	API_{30}
Spatially averaged CO_2 flux (10)	0.55	–0.50	0.52	0.59
Point 1–10 cm (8)	0.59	–0.51	0.66	0.40
20 cm (8)	0.54	–0.65	**0.74**†	0.47
30 cm (8)	0.43	–0.45	0.59	0.28
50 cm (8)	0.64	–0.42	0.56	0.28
Point 5–10 cm (8)	**0.74**†	**–0.74**†	**0.92***	**0.89***
20 cm (8)	0.66	–0.69	**0.85**††	**0.76**†
30 cm (8)	0.51	–0.67	**0.75**†	0.68
50 cm (8)	0.27	–0.39	0.51	0.51
Point 11–10 cm (7)	**0.82**†	–0.52	**0.82**†	0.68
20 cm (7)	0.53	–0.60	**0.75**†	0.51
30 cm (7)	0.51	–0.58	**0.75**†	0.48
50 cm (7)	0.71	–0.51	**0.81**†	0.61
Point 13–10 cm (7)	0.44	–0.58	**0.75**†	0.47
20 cm (7)	0.40	–0.52	**0.72**†	0.42
30 cm (7)	0.30	–0.33	0.56	0.20
50 cm (7)	0.15	–0.27	0.39	0.09
Point 15–10 cm (7)	**0.72**†	–0.68	**0.87***	**0.74**†
20 cm (7)	0.44	–0.27	0.66	0.48
30 cm (7)	0.63	–0.63	**0.88***	0.66
50 cm (6)	0.24	–0.14	0.33	–0.08

† $p < 0.05$, †† $p < 0.01$,* $p < 0.005$, and ** $p < 0.001$.

BGD
7, 6847–6887, 2010

Table 3. Continued.

(b) CH_4	VSWC	Soil temp.	30-day rainfall	API_{30}
Spatially averaged CH_4 flux (9)	0.41	–0.17	0.47	0.52
Point 1–10 cm (8)	–0.15	–0.11	0.17	0.06
20 cm (8)	0.24	–0.22	0.39	0.13
30 cm (8)	0.23	–0.24	0.48	0.10
50 cm (7)	–0.59	–0.23	–0.24	–0.48
Point 5–10 cm (8)	–0.68	0.11	**–0.75**†	–0.55
20 cm (8)	–0.68	–0.14	–0.37	–0.46
30 cm (8)	–0.60	–0.01	–0.53	–0.52
50 cm (8)	–0.54	–0.11	–0.39	–0.42
Point 11–10 cm (7)	0.04	–0.32	0.42	0.07
20 cm (7)	0.12	–0.09	0.39	–0.02
30 cm (7)	0.28	–0.21	0.50	0.11
50 cm (7)	0.23	–0.03	0.41	–0.06
Point 13–10 cm (7)	–0.33	–0.53	0.05	–0.21
20 cm (7)	–0.28	–0.39	0.14	–0.19
30 cm (7)	0.35	**–0.81**†	**0.80**†	**0.72**†
50 cm (7)	0.56	–0.46	0.71	0.41
Point 15–10 cm (7)	–0.05	0.12	0.12	–0.06
20 cm (7)	–0.64	–0.29	–0.40	–0.44
30 cm (7)	–0.14	0.17	–0.23	–0.53
50 cm (6)	0.31	**–0.91****	**0.77**†	0.73

† $p < 0.05$, $^{\dagger\dagger}p < 0.01$,* $p < 0.005$, and $^{**}p < 0.001$.

BGD
7, 6847–6887, 2010

Table 3. Continued.

(c) N_2O	VSWC	Soil temp.	30-day rainfall	API_{30}
Spatially averaged N_2O Flux (7)	**0.78***	**−0.75***	**0.78***	**0.97****
Point 1–10 cm (6)	0.65	−0.80	**0.85**†	**0.92**††
20 cm (6)	0.57	**−0.87**†	0.79	**0.84**†
30 cm (6)	0.48	−0.30	0.58	**0.82**†
50 cm (6)	0.61	−0.75	**0.84**†	**0.95***
Point 5–10 cm (6)	0.53	−0.71	**0.83**†	**0.92****
20 cm (6)	0.49	−0.70	0.80	**0.91***
30 cm (6)	0.42	−0.70	0.75	**0.87***
50 cm (6)	0.49	−0.72	0.81	**0.91***
Point 11–10 cm (5)	0.60	−0.74	**0.93**††	**0.96***
20 cm (5)	0.60	−0.76	**0.92**††	**0.96***
30 cm (5)	0.59	−0.78	**0.91**†	**0.95***
50 cm (5)	0.59	−0.75	**0.92**†	**0.96***
Point 13–10 cm (5)	0.58	−0.74	**0.94***	**0.89**†
20 cm (5)	0.53	−0.77	**0.92**†	**0.91**†
30 cm (5)	0.54	−0.77	**0.91**†	**0.93**††
50 cm (5)	0.39	**−0.81**†	0.79	**0.88**†
Point 15–10 cm (5)	0.58	−0.78	**0.93**††	**0.94**††
20 cm (5)	0.57	−0.78	**0.92**††	**0.93**††
30 cm (5)	0.55	−0.78	**0.92**††	**0.93**††
50 cm (4)	0.71	**−0.91**†	**0.99****	**0.98****

† $p < 0.05$, †† $p < 0.01$,* $p < 0.005$, and ** $p < 0.001$.

BGD
7, 6847–6887, 2010

Table 4. Pearson correlation coefficients and their levels of significance between gas flux and various environmental factors at each flux chamber on each sampling occasion. Figures in parentheses indicate the number of chambers on each sampling occasion. The values of volumetric soil water content (VSWC) were measured near each flux chamber immediately after the flux measurement.

Gas and measurement date	VSWC	N conc.	C conc.	C/N	VSWC and N conc.
CO_2 flux					
19 Aug 2006 (15)	−0.21	−0.01	−0.05	−0.11	0.21
3 Mar 2007 (39)	**−0.34**†	[a] −0.39	[a] −0.40	[a] −0.08	0.51
7 Mar 2007 (39)	**−0.32**†	0.07	0.06	0.02	0.32
12 Dec 2007 (39)	−0.11	0.07	0.07	0.03	0.11
16 Dec 2007 (39)	**−0.36**†	0.04	0.03	−0.02	0.24
6 Mar 2008 (39)	−0.23	0.07	0.03	0.02	0.23
9 Jun 2008 (39)	−0.12	0.27	0.12	−0.09	0.28
1 Oct 2008 (39)	0.02	0.06	0.03	0.03	0.06
9 Mar 2009 (39)	−0.22	0.26	0.25	0.10	0.37
14 Sep 2009 (39)	0.06	0.14	0.09	−0.02	0.16
10 obs. day average	−0.26	0.14	0.11	0.06	0.27
CH_4 flux					
19 Aug 2006 (15)	**−0.62**†	0.24	0.20	0.13	**0.67**†
3 Mar 2007 (39)	0.18	[a] −0.26	[a] −0.15	[a] 0.46	0.26
7 Mar 2007 (39)	**0.47***	−0.23	−0.24	−0.16	**0.85****
12 Dec 2007 (39)	0.11	0.13	0.06	−0.05	0.21
16 Dec 2007 (39)	**0.39**†	−0.05	−0.09	−0.06	**0.39**†
6 Mar 2008 (39)	**0.32**†	**−0.35**†	**-0.35**†	−0.31	**0.41**†
9 Jun 2008 (39)	0.29	−0.29	−0.28	−0.21	0.38
1 Oct 2008 (39)	0.18	0.23	0.18	−0.01	0.28
9 Mar 2009 (39)	0.04	−0.11	−0.10	0.00	0.13
9 obs. day average	**0.52****	0.04	−0.02	−0.11	**0.54***
N_2O flux					
19 Aug 2006 (15)	0.25	0.24	0.19	0.04	0.34
3 Mar 2007 (39)	0.02	[a] -0.24	[a] -0.21	[a] 0.10	0.24
12 Dec 2007 (39)	−0.07	0.21	0.28	**0.37**†	0.21
16 Dec 2007 (39)	0.20	0.26	0.27	0.27	**0.39**†
9 Jun 2008 (39)	0.27	0.27	0.16	−0.03	**0.41**†
1 Oct 2008 (39)	0.08	0.15	0.09	0.05	0.17
9 Mar 2009 (39)	−0.02	−0.04	−0.04	0.02	0.05
7 obs. day average	0.30	**0.40**†	**0.40**†	0.32	**0.55***

† $p < 0.05$, †† $p < 0.01$,* $p < 0.005$, and ** $p < 0.001$. [a] Nitrogen and carbon concentration in the soil was measured at 15 points along the frame of the 2-ha-plot.

BGD
7, 6847–6887, 2010

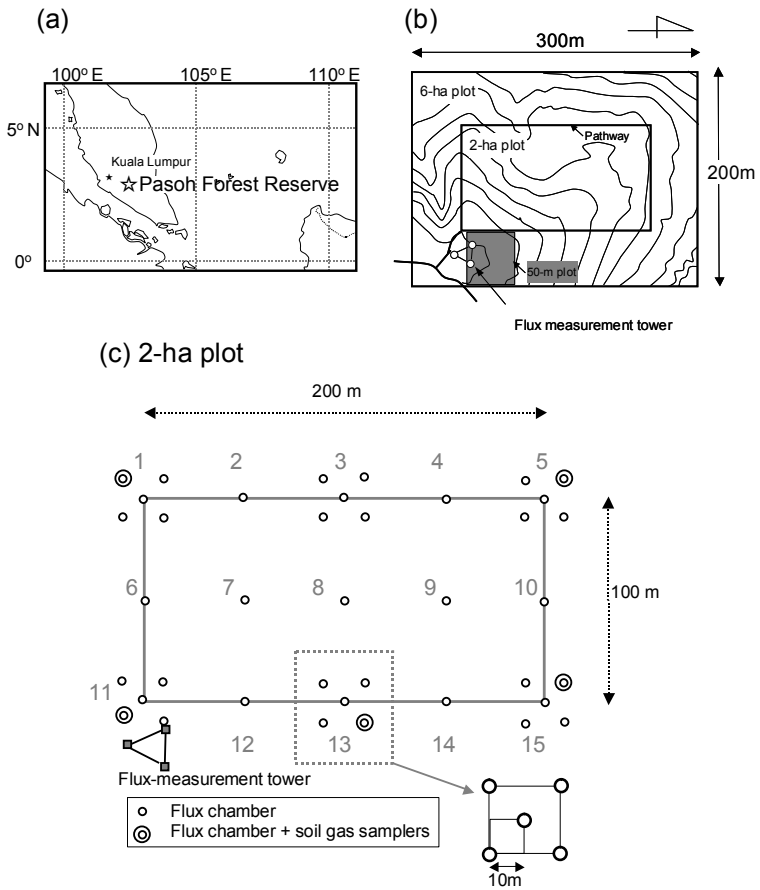

Fig. 1. **(a)** Location of the Pasoh Forest Reserve; **(b)** topographic map of the observation site in the Pasoh Forest Reserve; The contour interval is 1 m. **(c)** locations of the flux measurement chambers in the 2-ha study plot.

BGD
7, 6847–6887, 2010

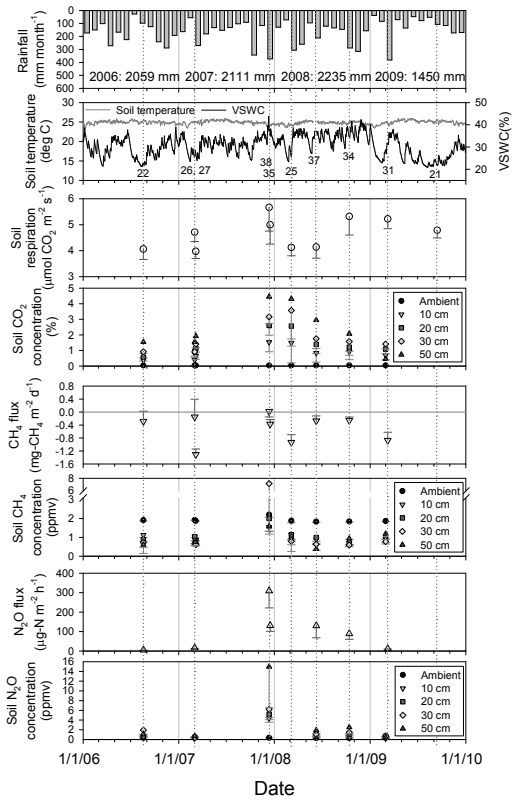

Fig. 2. Temporal variations in monthly rainfall, soil temperature, and soil volumetric water content (VSWC) at three points near the flux observation tower; CO_2 flux, soil CO_2 concentration, CH_4 flux, soil CH_4 concentration, N_2O flux, and soil N_2O concentration over time. Error bars indicate the standard error for all sampling chambers and tubes. The gray dashed lines indicate sampling dates. The numbers besides the VSWC line are the values of VSWC at the sampling times.

BGD
7, 6847–6887, 2010

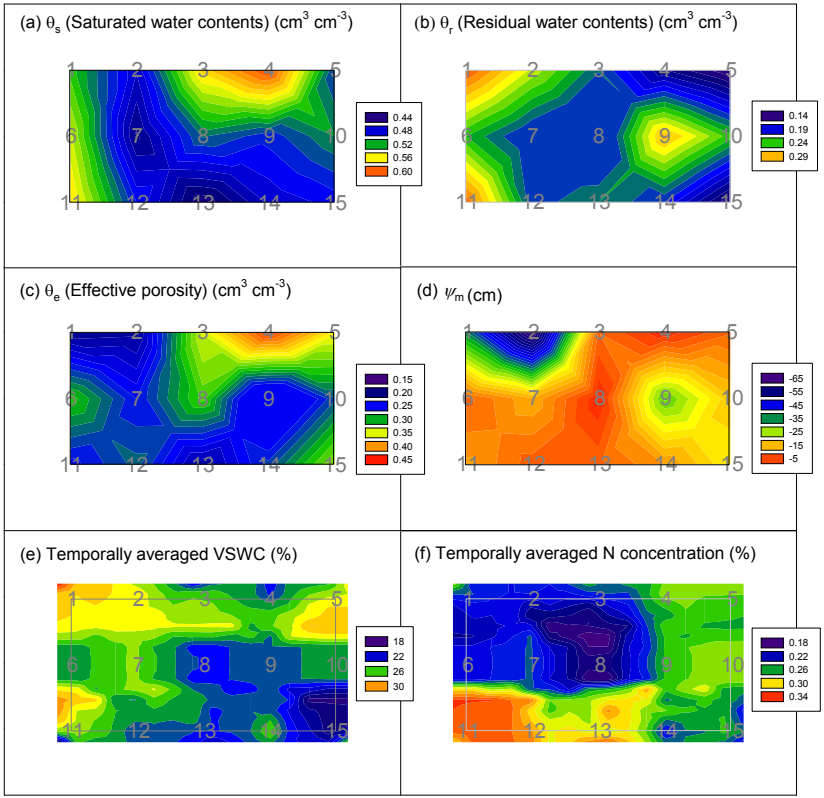

Fig. 3. The spatial distribution of **(a)** θ_s (saturated water content), **(b)** θ_r (residual water content), **(c)** θ_e (effective porosity), **(d)** ψ_m (the matric pressure head with respect to median pore radius), **(e)** temporally averaged soil volumetric water content (VSWC) measured adjacent to each chamber, and **(f)** temporally averaged soil N concentration in the study plot. The rectangular area represents the 2-ha plot shown in Fig. 1b and c, and the numbers in the figures indicate the positions of the 15 central sampling points.

BGD
7, 6847–6887, 2010

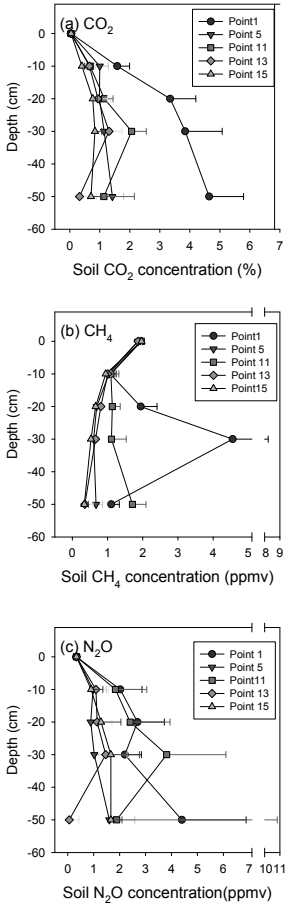

Fig. 4. Vertical profiles of soil CO_2, CH_4, and N_2O concentrations. Data are mean values of all sampling days for each sampling depth. Error bars indicate the standard error of concentrations observed on all sampling days.

BGD
7, 6847–6887, 2010

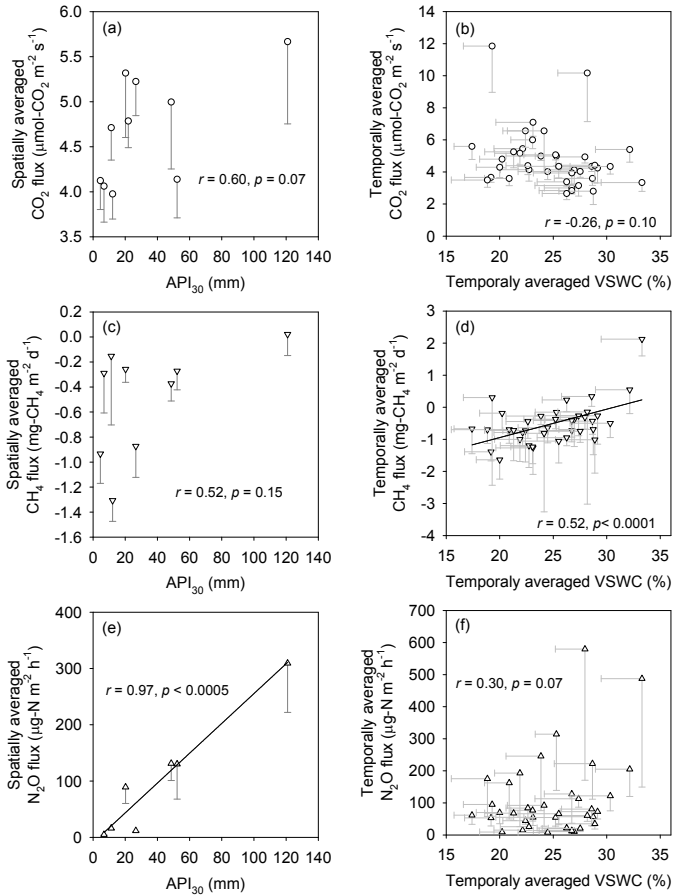

Fig. 5. Relationships between API_{30} and spatially averaged **(a)** CO_2 flux, **(c)** CH_4 flux, and **(e)** N_2O flux, and between temporally averaged VSWC and **(b)** CO_2 flux, **(d)** CH_4 flux, and **(f)** N_2O flux. Error bars indicate standard errors.

BGD
7, 6847–6887, 2010

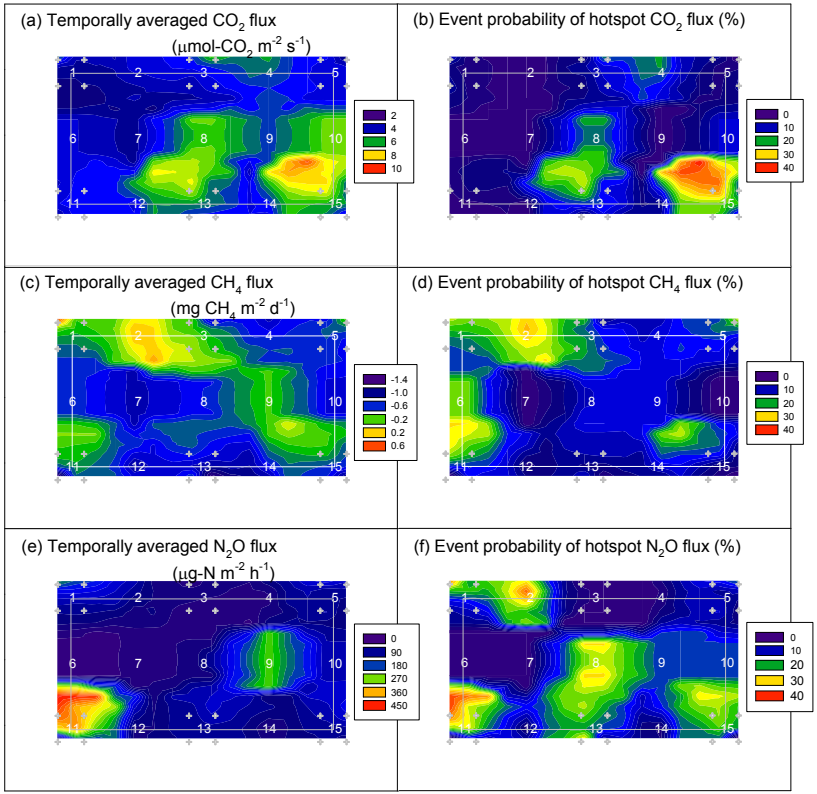

Fig. 6. The spatial distribution of temporally averaged **(a)** CO_2 flux, **(c)** CH_4 flux, and **(e)** N_2O flux, and the event probabilities of hotspots of **(b)** CO_2 flux, **(d)** CH_4 flux, and **(f)** N_2O flux. The rectangular area represents the 2-ha plot shown in Fig. 1b and c, and the numbers and cross symbols in the figures indicate the positions of the 15 central sampling points and their subpoints, respectively.

BGD
7, 6847–6887, 2010